

Aerocellulose Based on All-Cellulose Composites

Benoît J. C. Duchemin,¹ Mark P. Staiger,¹ Nick Tucker,² Roger H. Newman³

¹Department of Mechanical Engineering, University of Canterbury, Christchurch, New Zealand

²Food and Biomaterials Group, Plant and Food Research, Christchurch, New Zealand

³Bioproduct Development, Scion, Rotorua 3046, New Zealand

Received 9 April 2009; accepted 29 June 2009

DOI 10.1002/app.31111

Published online 27 August 2009 in Wiley InterScience (www.interscience.wiley.com).

ABSTRACT: Novel aerogels (or aerocellulose) based on all-cellulose composites were prepared by partially dissolving microcrystalline cellulose (MCC) in an 8 wt % LiCl/DMAc solution. During this process, large MCC crystals and fiber fragments were progressively split into thinner crystals and cellulose fibrils. The extent of the transformation was controlled by using cellulose concentrations ranging from 5 to 20 wt % in the LiCl/DMAc solution. Cellulose gels were precipitated and then processed by freeze-drying to maintain the openness of the

structure. The density of aerocellulose increased with the initial cellulose concentration and ranged from 116 up to 350 kg m⁻³. Aerocellulose with relatively high mechanical properties were successfully produced. The flexural strength of the materials reached 8.1 MPa and their stiffness was as high as 280 MPa. © 2009 Wiley Periodicals, Inc. *J Appl Polym Sci* 115: 216–221, 2010

Key words: all-cellulose composite; aerogel; WAXS; mechanical properties; microstructure

INTRODUCTION

Aerogels were first defined by Kistler as highly porous materials in which the liquid in a gel is replaced with one continuous gas phase.^{1,2} However, capillary action due to the liquid leaving the gel structure would result in collapse of the surrounding gel material. Thus, the highly porous structure of an aerogel is only achieved if the liquid is permitted to leave the gel as a gaseous phase via freeze- or supercritical drying. Aerogels are rigid, lightweight materials that are characterized by an extensive interconnected network of voids or pores that possess a very high surface to volume ratio. Hence, aerogels are found in a variety of applications including catalysts, fuel cell electrodes, cosmic dust collectors, insulation materials, and energy absorbers.^{2–5} Aerogels can be prepared from a broad range of materials ranging from silica to cellulose.^{2,4–6}

In particular, cellulose is well recognized as being a renewable and biodegradable natural polymer with high mechanical properties in its natural or derivatized forms and thus has potential for use in eco-friendly aerogels. Kistler, the inventor of aerogels, was also one of the first to create aerogels from

cellulose.¹ Following on from this, Tan et al. reported on the development of aerogels from cross-linked cellulose acetate and cellulose acetate butyrate via supercritical CO₂ drying.⁷ Following this, Fischer et al. recently developed a sol-gel route where cellulose acetate was crosslinked by urethane bonding and dried by supercritical CO₂ drying.⁸ Several researchers have also reported successful production of nonderivatized cellulose aerogels (also referred to as aerocellulose).^{6,9–14}

The preliminary step in creating an aerogel is to dissolve the cellulose. This is followed by precipitation in a suitable liquid media that acts to penetrate the structure and displace the solvent. For example, cellulose can be dissolved in aqueous calcium thiocyanate, precipitated in methanol, and then rinsed with deionized water.^{9,10} Another possible route involves the dissolution of cellulose in hydrated *N*-methylmorpholine *N*-oxide (NMMO) followed by a solvent exchange procedure involving heptane, water, acetone, methanol, or ethanol.^{6,13,14} Aerogels made of native cellulose dissolved in sodium hydroxide have also been reported.¹² Recently, two cellulose aerogels were prepared by dissolution of cellulose or lignocellulosic materials in ionic liquids.^{15,16} The final step in the preparation of an aerogel involves freeze-drying,^{9,10} supercritical drying,^{6,9,12–16} and sometimes drying by evaporation.¹¹ The choice of the drying method is critical to prevent the collapse of the cellulose pores.^{9,14}

This work attempts to merge the concepts of aerocellulose and all-cellulose composites with the aim of producing novel types of high strength and

Correspondence to: M. P. Staiger (mark.staiger@canterbury.ac.nz).

Contract grant sponsors: Biopolymer Network Ltd., Brian Mason Scientific, Technical Trust.

biodegradable aerogels. All-cellulose composites have recently been developed as a new class of biocomposite materials in which the microstructure consists of highly crystalline cellulose embedded in a matrix of regenerated cellulose.^{17–22} Here too, all-cellulose composites have some important advantages over other natural fiber biocomposites including greater compatibility between reinforcement and matrix, higher mechanical properties, and inherent biodegradability.^{17–20,22} In this work, all-cellulose composite aerogels have been synthesized via freeze-drying of cellulose gels obtained by partial dissolution of microcrystalline cellulose (MCC) using an 8.0 wt % LiCl/DMAc solvent system. The resulting aerocellulose was characterized in terms of density, microstructure, phase composition, and mechanical properties.

EXPERIMENTAL METHODS

Preparation of aerocellulose

Cellulose dissolution using *N,N*-dimethylacetamide (DMAc) initially involves an activation step in which the cellulose structure is first swollen via solvent exchange.^{21,23,24} The increased molecular mobility of cellulose after activation allows the LiCl/DMAc solvent to penetrate the cellulose structure more easily.^{25,26} In this work, MCC powder (Avicel, Merck, particle size range 20–160 μm) was activated by immersing in distilled water at 20°C for 48 h and vacuum-filtering through Whatman No. 1 filter paper, twice immersing in acetone (Biolab, laboratory grade) at 20°C for 24 h and filtering through Whatman No. 1 filter paper to remove the acetone each time, twice immersing in DMAc (Merck, synthesis grade) at 20°C for 24 h and each time filtering through Whatman No. 1 filter paper, vacuum-drying for 48 h at 60°C and finally passing the activated MCC through a sieve (90 μm). The activated MCC was vacuum-dried for a further 48 h at 60°C and finally sealed during storage. The degree of polymerization was 163 as determined using a method after Bianchi et al.²⁷

A solution of 8.0% (by total weight) LiCl in DMAc was prepared by mixing LiCl (Unilab, 99% purity, dried in a vacuum oven at 180°C overnight) and DMAc (Merck, synthesis grade, dried over 4 Å molecular sieve before use) in a 200 mL Schott bottle that was immediately sealed to minimize any moisture uptake. The mixture was mechanically stirred for 24 h to ensure that the LiCl was completely dissolved. Four grams of activated MCC was immersed under constant stirring in a small beaker containing sufficient LiCl/DMAc to achieve cellulose concentrations of $c = 5, 10, 15,$ and 20%, where c is expressed as a total percentage of cellulose on a weight basis.

The solutions were stirred for 3 min, poured in Petri dishes and placed under controlled atmosphere (20°C and 33% R.H.) for 24 h. A low humidity atmosphere was used to initiate gentle precipitation for improved shape retention of the gel. After the initial 24 h step, the gels were placed overnight at 76% R.H. and 20°C. At this stage, precipitation of the cellulose appeared to be complete. The precipitated cellulose was then thoroughly rinsed for 48 h under running tap water. The gels were then frozen overnight at –20°C. The gels were finally freeze-dried at –20°C and ~ 53 Pa for 48 h to produce samples of aerocellulose ~ 8 mm in thickness and 7–8 cm in diameter.

Materials characterization

X-ray patterns were obtained with a Philips PW1729 using a Cu target ($\lambda = 1.54040$ Å), voltage of 50 kV, and current of 40 mA over the range $5^\circ < 2\theta < 50^\circ$ in 0.02° steps. The samples were prepared as an ethanol/aerocellulose slurry mixture in an agate mortar using a pestle to mix the two components. This slurry was then applied to half a microscope slide and dried at room temperature. A crystallinity index (CrI) as defined by Segal et al. was used as a measure of the cellulose crystallinity.^{21,28} The measure was performed manually on graphs plotted from Microsoft Excel.

The bulk density of the aerocellulose was evaluated from the geometric dimensions and mass. Flexural mechanical testing of the aerocellulose was performed in accordance with ASTM-790. 3-point bend tests were conducted on an Instron Model 4444 (500 N load cell) at a crosshead speed of 10 mm/min. Samples were prepared 3–5 mm in height and 9–10 mm in width. A span of 35 mm was used between the sample supports. A minimum of five specimens were tested for each type of aerocellulose after conditioning for 40 h at $21 \pm 2^\circ\text{C}$ and $55 \pm 5\%$ R.H. The flexural strength (σ_f) and bending modulus (E_b) were normalized by the density, and the flexural strain to failure (ϵ_f) was recorded. Samples for field emission scanning electron microscopy (JEOL 7000F FE-SEM) were freeze-fractured, mounted on carbon tabs, gold coated (Emitech K975X High Vacuum Evaporator, 25 mA current, 0.2 bar of Ar pressure) and observed using an accelerating voltage of 3 kV.

RESULTS AND DISCUSSION

Wide-angle X-ray scattering

The relationship between initial cellulose concentration and phase composition in aerocellulose tended to follow the same trend as that observed for the all-cellulose composites. The nature of the phase

transformations during partial dissolution of MCC in 8 wt % LiCl/DMAc has been previously analyzed by wide-angle X-ray scattering (WAXS) and ^{13}C solid-state NMR.²¹ Partial dissolution of Avicel MCC involves the removal of sheets of cellulose from the surface of the initial cellulose I crystallites of the MCC. After precipitation and drying, the peeled cellulose sheets assemble into a mixture of amorphous and paracrystalline cellulose, resulting in a biphasic nanostructure. The amorphous and paracrystalline cellulose act as matrix in which large undissolved cellulose I crystals are embedded. ^{13}C solid-state NMR studies reveal a displacement of the C-4 peak and $T_2(\text{H})$ value that are sufficiently distinct from those observed for amorphous cellulose or highly crystalline cellulose I thus proving the existence of a paracrystalline phase.²¹ Paracrystalline cellulose produced in this work is a form of cellulose I with low crystallinity, analogous to cellulose IV₁ and sufficiently small to have all of the chains exposed to the surface. As a result of the phase transformations observed in MCC, the initial (200) peak is displaced from $2\Theta = 22.8^\circ$ to $2\Theta = 21^\circ$.²¹ The transformation of the original cellulose I crystallites into amorphous and paracrystalline phases tends to increase with decreasing cellulose concentration (c), while the CrI simultaneously decreases.

Similarly, for aerocellulose a second peak (200) at $2\Theta = 20.9^\circ$ associated with the paracrystalline matrix material progressively replaces the initial peak of strongly crystalline cellulose at $2\Theta = 22.8^\circ$ as c is decreased (Fig. 1)²⁹ while CrI decreases. CrI was measured to be 80% for activated MCC but decreased after dissolution to 67% for the composites prepared with $c = 20\%$; 55% with $c = 15\%$; 38% with $c = 10\%$; and 35% with $c = 5\%$. In accordance with decreasing CrI, the amount of paracrystalline matrix material created during partial dissolution increases. The crystalline (004) peak at $2\Theta = 35^\circ$ gradually disappears as c is decreased (Fig. 1) which is indicative of longitudinal disorder in the paracrystalline material.²¹ The CrI values reported here are about 10% lower than the values published for similar all-cellulose composites that were dried at a temperature of 60°C .²² The cellulose chains should indeed have less freedom to reassemble in an organized or paracrystalline fashion when they are locked in by ice crystals during drying. This phenomenon could account for the lower CrI of the all-cellulose composites that were obtained by freeze-drying.

Mechanical properties of aerocellulose

The densities of the aerocellulose were in the range of $120\text{--}350\text{ kg m}^{-3}$. For compositions with a higher c , and thus containing higher amounts of undissolved MCC, the density increased and was also

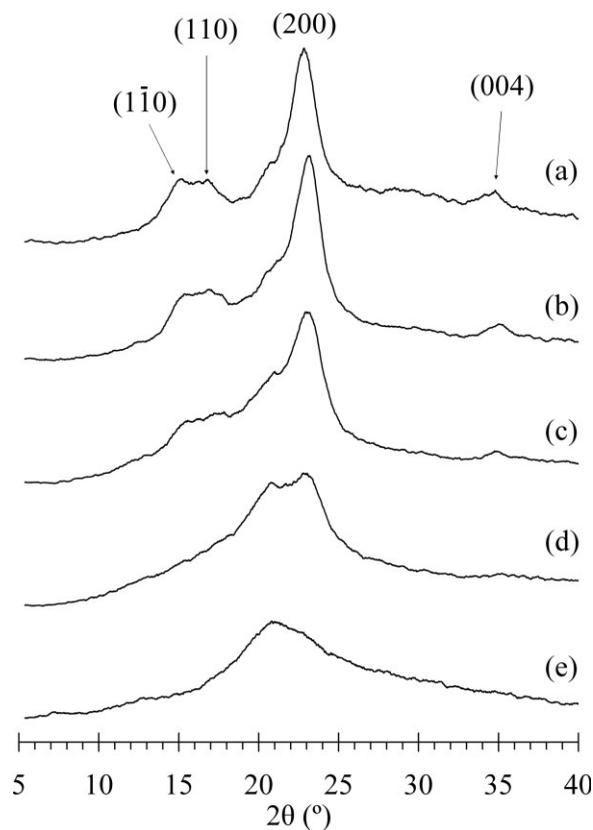


Figure 1 WAXS patterns of (a) activated MCC and all-cellulose composites prepared with (b) $c = 20\%$, (c) $c = 15\%$, (d) $c = 10\%$, and (e) $c = 5\%$. Peaks are assigned according to the monoclinic cellulose I unit cell after Sugiyama et al.²⁹

located in the higher end of the values normally encountered which range between 10 and 300 kg m^{-3} (Fig. 2).^{6,7,9,10,12,15,16} Initially, the gels that contain more cellulose per volume unit of LiCl/DMAc may be denser. The difference in density due to c persists through the entire precipitation, rinsing and freeze-drying process.⁶

The maxima in flexural strength and stiffness of 8.1 and 280 MPa, respectively, were obtained when $c = 10\text{--}15\%$ (Fig. 2). The observed maxima for this cellulose concentration are thought to be attributed to an optimal matrix to reinforcement ratio for a given material density. The specific flexural strength (σ_f) and specific stiffness (E_b) were also determined to take into account the highly variable density of aerocellulose (Fig. 3). σ_f and E_b monotonically increase with c , which demonstrates that the undissolved MCC plays an important role as a reinforcement. Whereas Hoepfner reported extremely ductile nanofibrillar aerocellulose,⁹ the material studied in this work was rather brittle and normally failed in tension.

The flexural strain to failure is a minimum for the intermediate concentrations ($c = 10\%$), although variation in ϵ_f was low over the concentration range

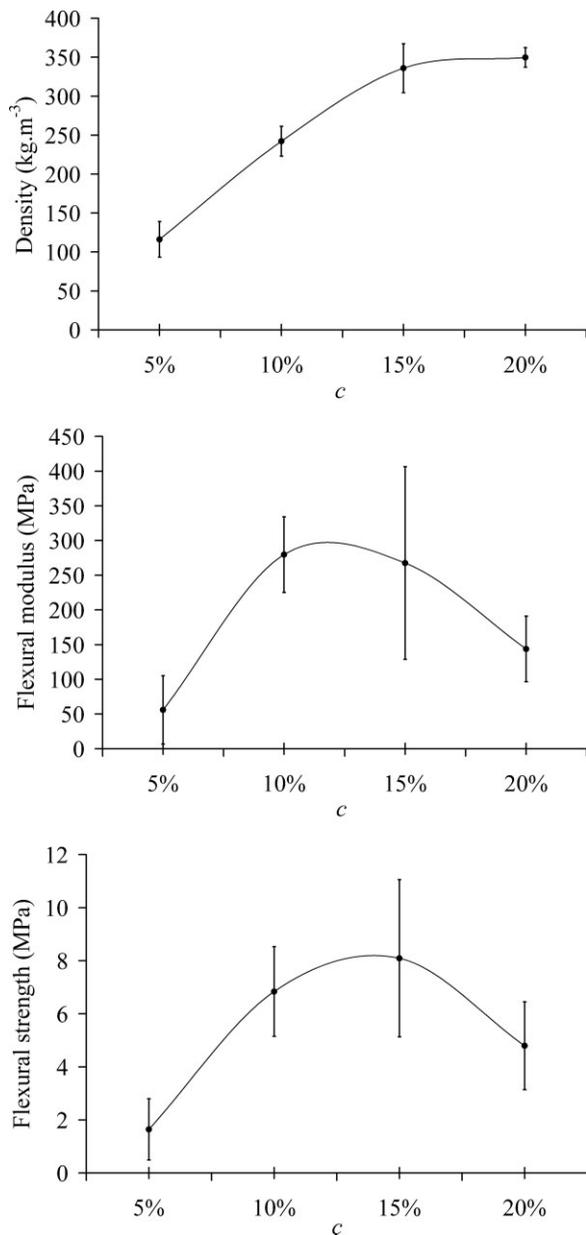


Figure 2 Density, Young's modulus, and flexural strength of aerocellulose prepared with $c = 5, 10, 15,$ and 20% .

studied. The amount of paracrystalline phase present in aerocellulose was increased with decreasing c (e.g., $c < 15\%$). Furthermore, low c allows more thorough dissolution which should lead to an aerocellulose with a more homogeneous and ductile microstructure. This was reflected in the higher strain to failure values at $c = 5\%$ (Fig. 3). Conversely, aerocellulose with a higher initial cellulose concentration (e.g., $c > 15\%$) contains a larger proportion of undissolved highly crystalline cellulose I which reduces the ductility of the aerocellulose (Fig. 3).

The freeze-fractured surfaces of aerocellulose typically exhibit a relatively smooth appearance when

the initial cellulose concentration is low with $c < 10\%$ [Fig. 4(a,b)]. As discussed, low c tends to produce a more homogeneous material due to the more thorough dissolution of the MCC fibrils which in turn leads to the regeneration of a paracrystalline phase with decreased longitudinal order.²¹ In contrast, when the cellulose concentration is increased, the fracture surfaces appear rougher that is indicative of fibril pull-out during fracture. Furthermore, the observed cellulose fibrils were $0.1\text{--}1\ \mu\text{m}$ wide which is consistent in scale with the as-received MCC. Concentrations of $c = 15\%$ yield composites with a fracture surface that are intermediate in terms of their roughness.

The increase in specific mechanical properties correlates with an increase in the crystallinity index (Figs. 1 and 3). A higher crystallinity also translates into a higher proportion of undissolved fibrils as observed directly on the freeze-fractured composite surfaces (Fig. 4). This trend in specific mechanical properties is expected since cellulose I is known to be stiffer than both its amorphous and paracrystalline counterparts. The Young's modulus of amorphous cellulose was calculated to be 10.42 ± 1.08 GPa by Chen et al.³⁰ Using X-ray diffraction, Nishino et al. measured the elastic modulus in the direction parallel to the chain axis of several cellulose polymorphs. Cellulose I was found to have a modulus of 138 GPa whereas cellulose IV₁, which is similar to the paracrystalline matrix material formed by partial dissolution, exhibited a value of 75 GPa.³¹ Ishikawa et al. published similar values and ranking of the mechanical properties of cellulose polymorphs based on ramie fiber.³² Hence, the changes in the specific Young's modulus also reflect the changes in the cellulose molecular structure and correlate with the changes in the CrI.

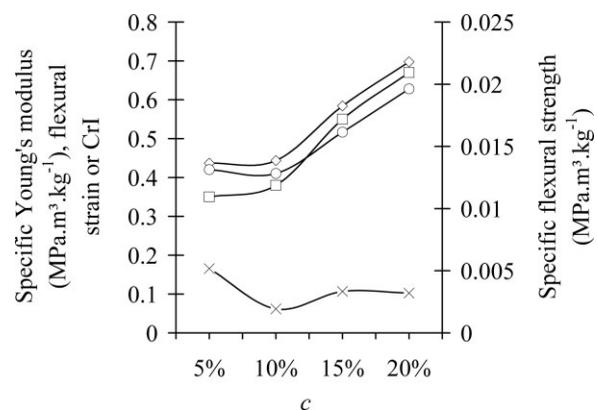


Figure 3 Graph showing the specific flexural strength (\circ), specific Young's modulus (\diamond), flexural strain (\times), and CrI (\square) of aerocellulose prepared with $c = 5, 10, 15,$ and 20% .

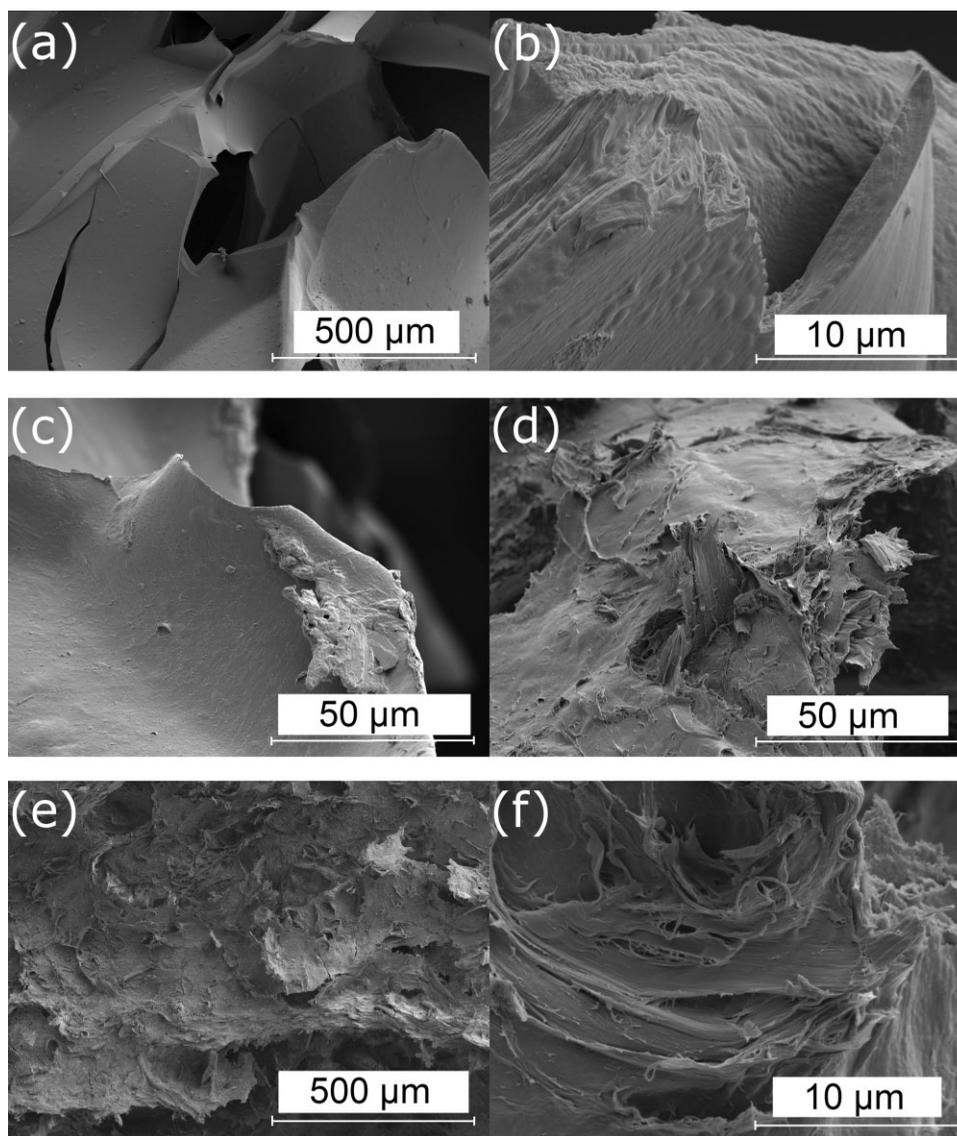


Figure 4 Scanning electron micrographs of freeze-fractured aerocellulose prepared with (a) and (b) $c = 5\%$, (c) $c = 10\%$, (d) $c = 15\%$, and (e) and (f) $c = 20\%$.

TABLE I
Mechanical Data for Examples of Low- to Medium-Density Organic Matter

| Foam | Density (kg m^{-3}) | Flexural strength (MPa) | Bending modulus (MPa) | Reference |
|----------------------------|--------------------------------|-------------------------|------------------------|-----------|
| Low density | | | | |
| Aerocellulose ^a | 115 | 17 | 480 | This work |
| Balsa | 60 | 7 (Tensile strength) | 2400 (Young's modulus) | 33 |
| EPS | 63 | 21 | 1670 | 34 |
| Starch | 120 | 13 | 810 | 34 |
| Corn starch | 130 | 18 | 1090 | 35 |
| Medium density | | | | |
| Aerocellulose ^b | 240 | 29 | 1170 | This work |
| Balsa wood | 200 | 130 (Tensile strength) | 7300 (Young's modulus) | 33 |
| Starch | 220 | 21 | 1280 | 34 |
| Wheat starch | 200 | 21 | 950 | 35 |
| Polypropylene | 297 | 18–24 | 740–1230 | 36 |

^a Data for $c = 5\%$.

^b Data for $c = 10\%$.

Comparisons with other foams

Published flexural properties (Table I) were selected for specimens with densities similar to those achieved in this work. In general, the aerocelluloses showed specific flexural strengths that were similar to other examples of low- to medium-density organic matter. The specific flexural modulus was lower than that for expanded polystyrene (EPS) foam, but was similar to values for balsa wood, starch foams, and polypropylene foam.

CONCLUSIONS

Aerocellulose was successfully produced by dissolving MCC in LiCl/DMAc, precipitating in water and followed by freeze-drying. The resulting aerocellulose exhibits a highly porous structure for which the density increases with the initial cellulose concentration c giving rise to a family of materials with different mechanical characteristics. Overall, the consolidation mechanism is thought to involve the following steps:

- During dissolution in LiCl/DMAc, cellulose layers are peeled away from the crystals and form aggregates in solution. Those aggregates are precipitated by exposure to water. In the final material, they consolidate in a paracrystalline matrix that binds the larger cellulose crystals together. The amount of paracrystalline material is inversely proportional to c .
- The MCC fibrils are broken down into a paracrystalline matrix and split into smaller fibrils. For low cellulose concentrations ($c < 10\%$), the initially large MCC crystallites are almost completely replaced by a paracrystalline phase. Conversely, the materials with a high cellulose concentration ($c > 15\%$) exhibit a relatively different morphology where a large portion of the microstructure consists of fibrils that are consistent in scale with the original nondissolved MCC or cellulose fibrils.

Generally, the specific flexural strength and stiffness increase with the content of highly crystalline cellulose. The flexural properties are similar to those of other examples of low- to medium-density organic matter. Aerocellulose is a bio-based, biodegradable, and environmentally friendly alternative to synthetic foams, with applications ranging from structural foams to packaging.

The authors thank K. Stobbs for help with materials preparation, M. Flaws and M. Kral for SEM sample preparation,

S. Brown for acquisition of the WAXS patterns, and K. Denizot for the DP work.

References

1. Kistler, S. S. *J Phys Chem* 1932, 36, 52.
2. Kistler, S. S. U.S. Pat. 2,093,454 (1937).
3. Hrubesh, L. W. *J Non-Cryst Solids* 1998, 225, 335.
4. Burchell, M. F.; Graham, G.; Kearsley, A. *Annu Rev Earth Planet Sci* 2006, 34, 385.
5. Guilminot, E.; Fischer, F.; Chatenet, M.; Rigacci, A.; Berthon-Fabry, S.; Achard, P.; Chainet, E. *J Power Sources* 2007, 166, 104.
6. Innerlohinger, J.; Weber, H. K.; Kraft, G. *Macromol Symp* 2006, 244, 126.
7. Tan, C.; Fung, B. M.; Newman, J. K.; Vu, C. *Adv Mater* 2001, 13, 644.
8. Fischer, F.; Rigacci, A.; Pirard, R.; Berthon-Fabry, S.; Achard, P. *Polymer* 2006, 47, 7636.
9. Hoepfner, S.; Ratke, L.; Milow, B. *Cellulose* 2007, 15, 121.
10. Jin, H.; Nishiyama, Y.; Wada, M.; Kuga, S. *Colloids Surf A: Physicochem Eng Aspects* 2004, 240, 63.
11. Khare, V. P.; Greenberg, A. R.; Kelley, S. S.; Pilath, H.; Roh, I.; Tyber, J. *J Appl Polym Sci* 2007, 105, 1228.
12. Gavillon, R.; Budtova, T. *Biomacromolecules* 2008, 9, 269.
13. Liebner, F.; Haimer, E.; Potthast, A.; Loidl, D.; Tschegg, S.; Neouze, M.-A.; Wendland, M.; Roseneau, T. *Holzforchung* 2009, 63, 3.
14. Liebner, F.; Potthast, A.; Rosenau, T.; Haimer, E.; Wendland, M. *Holzforchung* 2008, 62, 129.
15. Aaltonen, O.; Jauhiainen, O. *Carbohydr Polym* 2009, 75, 125.
16. Tsiptsias, C.; Stefopoulos, A.; Kokkinomalis, I.; Papadopoulou, L.; Panayiotou, C. *Green Chem* 2008, 10, 965.
17. Nishino, T.; Matsuda, I.; Hirao, K. *Macromolecules* 2004, 37, 7683.
18. Gindl, W.; Keckes, J. *Polymer* 2005, 46, 10221.
19. Gindl, W.; Schoberl, T.; Keckes, J. *Appl Phys A: Mater Sci Process* 2006, 83, 19.
20. Nishino, T.; Arimoto, N. *Biomacromolecules* 2007, 8, 2712.
21. Duchemin, B.; Newman, R.; Staiger, M. *Cellulose* 2007, 14, 311.
22. Duchemin, B. J. C.; Newman, R. H.; Staiger, M. P. *Compos Sci Technol* 2009, 69, 1225.
23. Dupont, A.-L. *Polymer* 2003, 44, 4117.
24. Striegel, A. M. *J Chil Chem Soc* 2002, 48, 73.
25. Ishii, D.; Tatsumi, D.; Matsumoto, T. *Biomacromolecules* 2003, 4, 1238.
26. McCormick, C. L.; Callais, P. A.; Hutchinson, B. H. *Macromolecules* 1985, 18, 2394.
27. Bianchi, E.; Ciferri, A.; Conio, G.; Cosani, A.; Terbojevich, M. *Macromolecules* 1985, 18, 646.
28. Segal, L.; Creely, J. J.; Martin, A. E., Jr.; Conrad, M. C. *Text Res J* 1959, 29, 786.
29. Sugiyama, J.; Vuong, R.; Chanzy, H. *Macromolecules* 1991, 24, 4168.
30. Chen, W.; Lickfield, G. C.; Yang, C. Q. *Polymer* 2004, 45, 1063.
31. Nishino, T.; Takano, K.; Nakamae, K. *J Polym Sci Part B: Polym Phys* 1995, 33, 1647.
32. Ishikawa, A.; Okano, T.; Sugiyama, J. *Polymer* 1997, 38, 463.
33. Wegst, U. G. K.; Ashby, M. F. *Philos Mag* 2004, 84, 2167.
34. Glenn, G. M.; Orts, W. J.; Nobes, G. A. R. *Ind Crops Prod* 2001, 14, 201.
35. Shey, J.; Imam, S. H.; Glenn, G. M.; Orts, W. J. *Ind Crops Prod* 2006, 24, 34.
36. Hwang, J.-J.; Adachi, T.; Kuwabara, T.; Araki, W. *Mater Sci Eng* 2007, 487, 369.